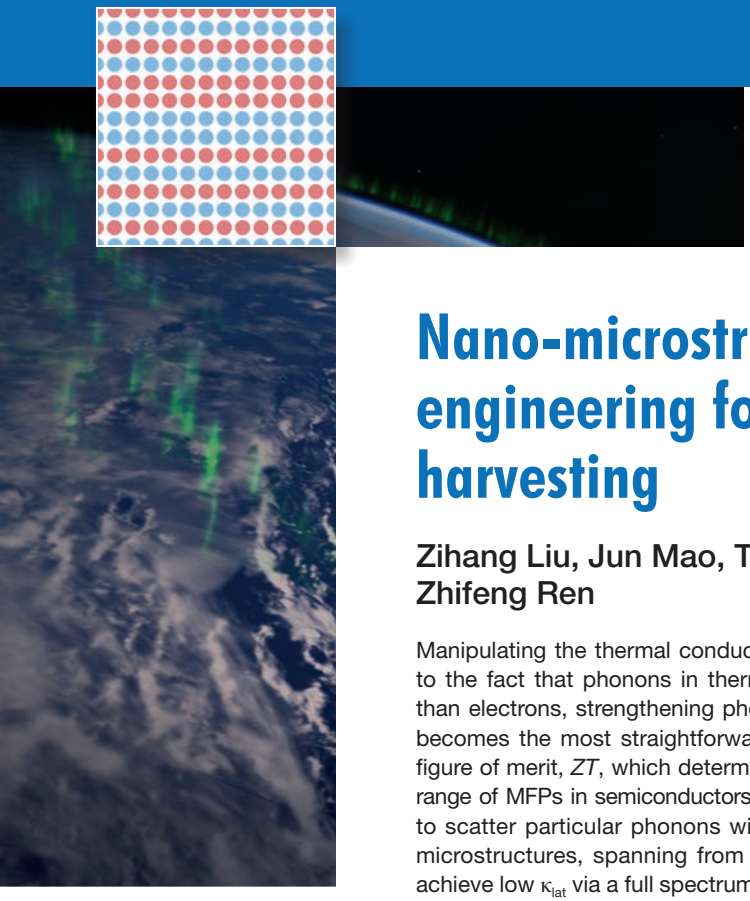


Nano-microstructural control of phonon engineering for thermoelectric energy harvesting

Zihang Liu, Jun Mao, Te-Huan Liu, Gang Chen, and Zhifeng Ren

Manipulating the thermal conductivity of solids is important for practical applications. Due to the fact that phonons in thermoelectric materials have longer mean free paths (MFPs) than electrons, strengthening phonon scattering to reduce lattice thermal conductivity (κ_{lat}) becomes the most straightforward and effective approach to enhance the thermoelectric figure of merit, *ZT*, which determines the maximum device efficiency. Phonons have a wide range of MFPs in semiconductors, and different dimensions of lattice defects can be targeted to scatter particular phonons with distinct relaxation times. Designing hierarchical nano-microstructures, spanning from point defects to volume defects, would be beneficial to achieve low κ_{lat} via a full spectrum of phonon scattering. Herein, we review the formation and underlying mechanisms for lattice defects and highlight the role of all-scale hierarchical nano-microstructure on phonon engineering. Existing challenges in simulations are also discussed.

Introduction

Manipulating thermal-transport properties is important for various applications ranging from integrated circuits and optoelectronics to thermoelectric energy conversion.[1,2] Thermoelectric generators, capable of realizing direct energy conversion from heat into electricity, are solid-state devices with broad future promise for low-grade waste heat harvesting. The conversion efficiency is dominated by the material's dimensionless thermoelectric figure of merit:

$$ZT = \left(S^2\sigma/\kappa\right)T, \tag{1}$$

where S, σ, κ, and T are the Seebeck coefficient, electrical conductivity, total thermal conductivity (including contributions from lattice, κ_{lat} , and electrons, κ_{el}), and absolute temperature, respectively. For more than a half century, a *ZT* of approximately 1 has been generally considered as the benchmark for pursuing high *ZT*.

Stimulated by the concept of "quantum confinement" coupled with the introduction of advanced synthesis techniques,[3,4] a series of record-high *ZT* values have been realized for materials and structures ranging from quantum dots (zero-dimensional structures) to bulk nanostructured materials (three-dimensional [3D] structures) over the past two decades.[5–7] These critical advances are mainly attributed to reduced κ_{lat}, since κ_{lat} is relatively independent of the electronic properties.[8] Generally, heat conduction in a semiconductor is mostly dominated by lattice vibrations, which can be approximately understood using kinetic theory:

$$\kappa_{lat} = \frac{1}{3}C_v v l, \tag{2}$$

where C_v is the specific heat of the semiconductor, v is the phonon group velocity, and l is the phonon mean free path (MFP). Heat transport in thermoelectric materials results from the cumulative contributions of phonons with a broad range of MFPs, and different MFPs contribute different amounts to κ_{lat} for a specific material.[9] Taking bulk crystalline silicon as a representative example, its MFP spectrum spans more than five orders of magnitude from 1 nm to 100 μm at room temperature.[10] Thus, designing multiscale microstructures encompassing point defects, linear defects, interfacial defects, and volume defects could scatter phonons across a wide range of length scales, maximally suppress κ_{lat}, and thereby increase *ZT*.[11–14]

Zihang Liu, Department of Physics, University of Houston, USA; zliu48@central.uh.edu
Jun Mao, Department of Mechanical Engineering, University of Houston, USA; jmao5@uh.edu
Te-Huan Liu, Department of Mechanical Engineering, Massachusetts Institute of Technology, USA; thliu@mit.edu
Gang Chen, Department of Mechanical Engineering, Massachusetts Institute of Technology, USA; gchen2@mit.edu
Zhifeng Ren, Department of Physics, University of Houston, USA; zren@uh.edu
doi:10.1557/mrs.2018.7

© 2018 Materials Research Society

https://doi.org/10.1557/mrs.2018.7 Published online by Cambridge University Press

For practical applications of thermoelectric materials, bulk nanostructured materials hold great promise for commercialization due to their practicability, compared to quantum dots, nanowires, and superlattices.[15] By designing special nano-microstructures to tailor thermal conductivity, we have witnessed great progress in bulk high-performance materials for thermoelectric applications, especially boosting large-scale energy-harvesting applications. In this article, we provide an overview of the reasons for the formation of as well as phonon-scattering mechanisms of microstructural defects, highlight the role of hierarchical microstructures and point out challenges in related simulations.

Phonon engineering via microstructural defects

Real materials are not perfect, and defects will inevitably scatter phonons. Phonon MFP or relaxation time, τ, depends upon phonon scattering by microstructural defects in addition to intrinsic phonon–phonon scattering. Manipulating phonon transport by designing defects is feasible. **Figure 1** shows schematic diagrams and corresponding high-resolution transmission electron microscope images of common defects in solids.[12,14,16–18]

Point defects are usually thermodynamically stable due to the balance between increased crystal distortion energy and system entropy;[19] these include vacancies, interstitials, and impurity atoms. Vacancies are the primary intrinsic point defects owing to their low formation energy.[19] Tuning the stoichiometric composition or extrinsic methods (e.g., radiation treatment) can control the vacancy concentration in semiconductors.[20,21] Interstitials are high-energy defects that are less common than other point defects.[19] In some cases, small atoms tend to occupy octahedral or tetrahedral interstitial sites of a cubic lattice or van der Waals gaps of lamellar structures.[22] In thermoelectric materials, impurity atoms are more common due to the requirement of decreasing the thermal conductivity or optimizing the carrier concentration. Antisite defects may also occur in an ordered alloy or compound (e.g., Bi locating to Te sites in Bi_2Te_3).[23]

Phonon scattering by point defects mainly arises from mass and strain fluctuations.[24] Vacancies and interstitials, which are considered the strongest phonon-scattering centers, can maximize these fluctuations. Rattling fillers in skutterudites, which have the general formula RM_4X_{12} (R is normally rare-earth elements, M is Fe, Ru, or Os, and X is P, As, or Sb), could effectively reduce κ_{lat} due to resonant scattering and other factors, for example, the reduced group velocity of phonons.[25] However, the concentration of defects plays a critical role in the phonon–impurity coupling strength, and therefore, isoelectronic substitution could dramatically suppress κ_{lat}, especially for heavy elements.[26]

Linear defects or dislocations were first introduced to explain the low fracture strength of real materials.[27] Plastic deformation is the most commonly used method to increase the dislocation density in metal.[28] Due to the low density of dislocations at equilibrium in semiconductors, phonon scattering by dislocations has long been overlooked in thermoelectrics.

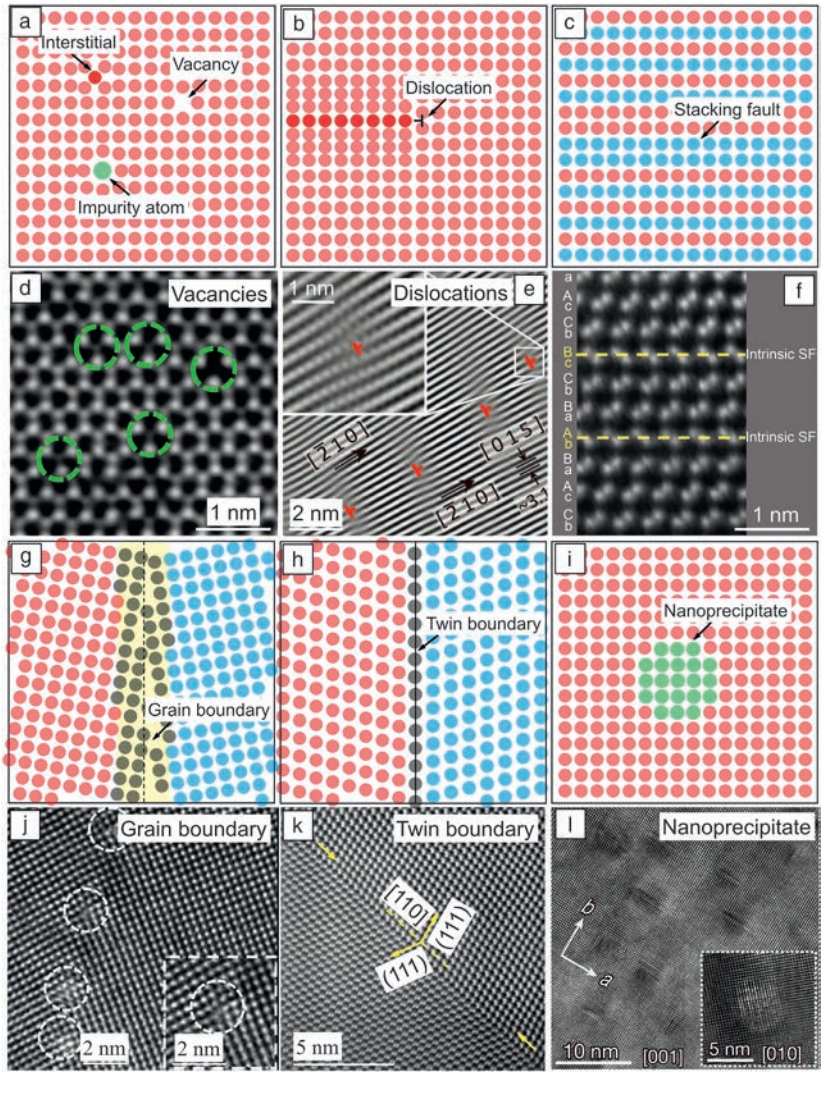


Figure 1. Schematic diagrams and corresponding high-resolution transmission electron microscope images of common defects in solids. (a, d) Vacancies. Reprinted with permission from Reference 16. © 2015 Nature Publishing Group. (b, e) Dislocations. Reprinted with permission from Reference 14. © 2015 AAAS. (c, f) Stacking faults (SFs).[18] (g, j) Grain boundaries. Reprinted with permission from Reference 17. © 2014 Wiley. (h, k) Twin boundaries.[18] (i, l) Nanoprecipitates. Reprinted with permission from Reference 12. © 2012 Nature Publishing Group. The insets in (e), (j), and (l) show the morphology of a dislocation, dislocation (on the grain boundary), and nanoprecipitate, respectively.

https://doi.org/10.1557/mrs.2018.7 Published online by Cambridge University Press

Recently, liquid-phase compaction was used to produce low-angle grain boundaries with dense dislocation arrays, as demonstrated in $Bi_{0.5}Sb_{1.5}Te_3$ and Yb-filled $CoSb_3$.[14,29] Dislocation loops can be generated by the collapse of vacancy discs in lead chalcogenides,[30,31] which was initially observed in metals.[32]

A dislocation consists of a core and an elastic stress field, hence in principle, phonon scattering via dislocations can have two distinctive mechanisms.[33] Scattering via dislocation cores can be considered a short-range-interaction model similar to mass-difference impurity scattering, whereas phonon scattering via the elastic field shows long-range characteristics that depend on the type of dislocation.[33] Recently, the concept of a "dislon," a quantized quasiparticle of dislocation that can interact with elastic waves, has been used to explore the nonperturbative nature of coupling between a dislocation and a phonon.[34]

Interfacial defects mainly include grain boundaries, stacking faults, and twin boundaries. Several nonequilibrium approaches, such as high-energy ball milling or melting spinning, in combination with quick direct-current hot press or spark plasma sintering, could be used to fabricate nanostructured materials with a high density of grain boundaries.[11,35–37] Stacking faults and twin boundaries are usually related to solid-state phase transformations (e.g., GeTe alloys)[38] or close-packed crystal structures with low formation energy (e.g., copper-based materials).[39,40] Stacking faults or twin boundaries can also be observed after heavy plastic deformation[18,41] and develop due their lower formation energies than normal grain boundaries.[42]

Qualitatively speaking, the phonon–boundary scattering rate by interfacial defects is evaluated by the boundary misfit angle, namely coherent, semicoherent, and incoherent.[43] For example, the phonon relaxation time has an inverse correlation with the square of the grain-boundary misfit angle for low-angle grain boundaries.[43] Thus, stacking faults, twin boundaries, and low-angle grain boundaries have a smaller impact on thermal transport compared to conventional high-angle grain boundaries as they do not reflect phonons effectively. Given the microstructural complexity and other unknowns, it is difficult to give a quantitative picture of scattering strength in bulk materials merely based on experiments. Nevertheless, detailed computations have provided a clear microscopic understanding of phonon scattering by interfacial defects in specific systems (e.g., SiGe alloys).[44]

Volume defects are 3D aggregates of atoms or vacancies, including precipitates and voids. Traditional metallurgical science (e.g., nucleation and growth or spinodal decomposition) enables better understanding and control of the morphology, size, and density of precipitates in the matrix.[45] Nucleation and growth methods require low or no precipitate solubility in the solid state, but complete solubility in the liquid state. Due to the final increased system free energy, interfacial energy and strain energy codetermine the final morphology of a precipitate.

Here, it should be mentioned that $AgPb_mSbTe_{2+m}$, known as the LAST alloy, has endotaxially embedded Ag-Sb–rich nanoprecipitates, resulting in a ultrahigh *ZT* of ~2.2 at 800 K.[46] This strongly motivated the development of nanostructured thermoelectric materials with *in situ* nanoprecipitates.[47–49] Spinodal decomposition, having a miscibility gap in the phase diagram, is a typical "uphill" diffusion process without the requirement to overcome the thermodynamic barrier, leading to the formation of a uniform-sized, periodic fine microstructure. More importantly, the phase interfaces generally remain coherent or semicoherent; meanwhile, the separate regions with the same crystal structure only hold different chemical compositions.[45] Specifically, PbTe/GeTe, PbTe/PbS (Ti, Zr, Hf) NiSn, and $La_{0.8}Ti_{0.1}Ga_{0.1}Fe_3CoSb_{12}$, show the typical morphology of spinodal decomposition,[50–54] but there are few concrete investigations on the role of spinodal decomposition in phonon scattering.

Recently, it was found that in *p*-type filled skutterudites with spinodal decomposition, the sharp reduction in κ_{lat} is caused by the strain-field scattering of high-energy phonons.[52] In certain circumstances, some nanoscale second phases (e.g., SiC,[55] carbon nanotubes,[56] and reduced graphene oxide[57]) are also intentionally incorporated into the parent phase to suppress κ_{lat} or enhance mechanical properties. For porous structures, the reduction in κ_{lat} depends not only on the volume fraction of pores, but also on their aspect ratio and spatial distribution.[58] Normally, the existence of low volatile phases or a hollow precursor forms a porous 3D structure,[59] but the validity of enhancing *ZT* is still in debate owing to the counterbalancing effect of degrading electrical conductivity.[60] Recently, a porous architecture containing nano- to micrometer-size irregularly shaped and randomly oriented pores in rare-earth-free skutterudites, $\sim Co_{23.4}Sb_{69.1}Si_{1.5}Te_{6.0}$, was shown to give rise to a high $ZT \sim 1.6$, showing more than a 100% increase as compared to the pristine sample.[61]

For phonon scattering via spherical nanoprecipitates, the relaxation time interpolates between long (geometrical scattering) and short (Rayleigh limit) wavelength scattering regimes. For the scattering cross section, the mass or force constant between nanoprecipitates and matrix dominates in the Rayleigh limit while the path length and the associated phase lag matter in the near geometrical scattering regime.[62] Kundu et al. pointed out the different roles of lighter and heavier nanoprecipitates in phonon scattering, where higher scattering rates can be achieved for heavier nanoprecipitates at low frequencies.[63] For the best distribution of spherical nanoparticles, previous calculations show that large size distributions block broad-spectrum phonon transport.[62] Zhang et al. recently reported that a discrete size distribution at a few well-chosen radii will be more effective.[64] For nanoparticles with other shapes, a qualitative description for phonon scattering could be achieved by means of more elaborate treatments due to the complexity of the geometry.[65]

The critical role of hierarchical micro-/nanostructures

Recently, both theoretical and experimental results on semiconductors have proven that phonons with a broad MFP

https://doi.org/10.1557/mrs.2018.7 Published online by Cambridge University Press

spectrum contribute to κ_{lat}.[9,66] Nano-microstructural defects with different dimensions are targeted to scatter phonons of comparable sizes. The effective scattering rate τ_{eff}^{-1} can be evaluated by Matthiessen's rule, which assumes scattering channels are independent of each other: $\tau_{eff}^{-1} = \sum_I \tau_I^{-1}$, where τ_I^{-1} represents the relaxation time of a specified type of defect I.[67,68]

Different defects have different phonon-scattering rates. Point defects have a phonon-scattering rate $\tau_{PD}^{-1} \sim \omega^4$, where ω is phonon frequency, thus showing they are preferable to scattering the phonons with high frequencies that could be analogous to Rayleigh scattering. Dislocations act as scattering centers mainly for mid-frequency phonons, where the phonon-scattering rates arising from the dislocation core and strain field are given by $\tau_{DC}^{-1} \sim \omega^3$ and $\tau_{DS}^{-1} \sim \omega$, respectively. The grain-boundary scattering rate is independent of phonon frequency, $\tau_{GB}^{-1} \sim \omega^0$, when the misfit angle is less than 15° and has stronger interactions with low-frequency phonons.

Apart from these scattering centers, nanoprecipitates could scatter phonons in a wider frequency range, $\tau_{NP}^{-1} \sim \omega^0 + \omega^4$. Therefore, a large suppression of κ_{lat} could be realized by hierarchical micro-/nanostructures due to the scattering of phonons over broad frequencies.[12] This strategy was first proposed in the PbTe-SrTe system that includes atomic-scale lattice disorder, nanoscale endotaxial precipitates, and microscale grain boundaries, which pushes ZT to greater than 2.[12] This strategy is also applicable to other material systems (e.g., α-MgAgSb[69,70]) and can accelerate breakthroughs in thermoelectric science.[37,71]

Challenges

It is now generally recognized that the defects previously discussed are important tools for improving ZT, however, simulation tools are not yet at a level to guide the rational design of defects. The improvements in ZT so far are mostly based on trial and error. Some key challenges from a simulation and modeling perspective are discussed here.

First-principles simulation of electron transport

Ideally, one would design nanostructures such as grain size to be in between electron and phonon MFPs such that interfaces scatter more phonons than electrons. Knowing the MFP distributions of electrons and phonons in intrinsic materials is thus important. Although first-principles-based phonon simulation tools are becoming mature,[10] electron simulation tools are just becoming available since the recent development of Wannier interpolation, a complete set of orthogonal functions used in solid-state physics, for electron–phonon coupling matrices.[72,73] There are limited reports on fully first-principles-based simulations of electron thermoelectric transport properties, although simulations based on the constant relaxation time approximation are routinely reported.[74] In **Figure 2**, we compare electron and phonon MFP distributions in several representative materials.[66,75–79] More detailed studies show that nanostructures can also be effective for manipulating phonon and electron transport in some materials even when they are comparable to both the electron and phonon MFPs, since some long MFP electrons are disadvantageous to the Seebeck coefficient.[15]

First-principles simulation of defects scattering of phonons and electrons

Defects clearly affect phonon thermal conductivity; however, interpretations of experimental data to date are based on phenomenological models pioneered by Klemens and Callaway.[67,68] Classical models, for example, cannot explain the interface resistance.[80] Progress has been made in simulating interfacial thermal resistance based on the nonequilibrium atomic Green's function and molecular dynamics.[44,81] Simulations show that even atomic-point defects cannot be well described by Rayleigh scattering except in the long phonon wavelength range. For electron transport, critical questions remain about the charging states of these defects and how they contribute to carriers, as they can donate or trap mobile carriers.[82] Knowing the charging states will enable answering the next question—how do these defects scatter electrons? Despite past studies on electrons in electronics and photonics, the current tools are far from being able to treat electron defect scattering on a first-principles basis.

Multiscale simulation of hierarchical defects

Although progress is being made on treating individual defects, putting them together to simulate realistic materials with hierarchical defects remains a major challenge. Appropriate methods to average the individual defect's contribution and to bridge the scales are yet to be developed.

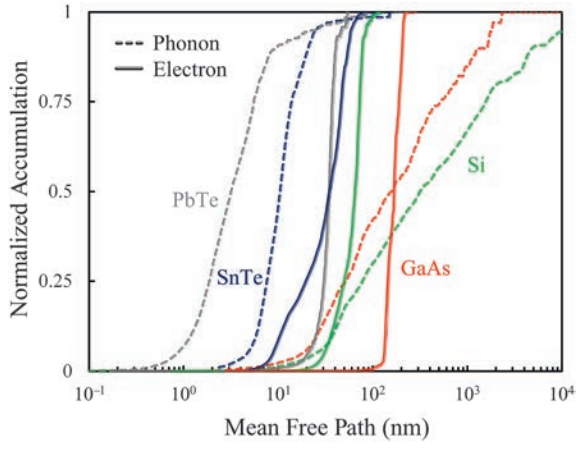


Figure 2. Normalized accumulation of thermal (dashed) and electrical conductivity (solid lines) for four representative materials. The blue, red, green, and gray lines represent the mean free path (MFP) spectra of SnTe,[78] GaAs,[76,77] Si,[10] and PbTe,[66,79] respectively. The electrical conductivities are calculated at an n-type carrier concentration of 1×10^{20}, 1×10^{13}, 1×10^{14}, and 1×10^{17} cm^{-3} for SnTe, GaAs, Si, and PbTe, respectively. The differences between phonon and electron MFPs provide the possibility to independently manipulate their transport behavior.

https://doi.org/10.1557/mrs.2018.7 Published online by Cambridge University Press

Conclusions and outlook

In this article, we summarized the formation conditions and phonon-scattering mechanisms of nano-microstructural defects in bulk thermoelectric materials, ranging from point defects to volume defects. The role of all-scale hierarchical nano-microstructures on impeding phonon transport is highlighted. We also discussed the main challenges for the roles of defects or microstructure from the perspective of simulations.

The thermal stability of nonequilibrium defects may become a critical issue during long-term practical applications. In addition to phonon engineering by defects, it is essential to pay attention to the effects of carrier concentration and carrier-scattering mechanisms,[83,84] which may counteract the beneficial contributions of the phonon portion and even deteriorate the final *ZT*. Therefore, delicate manipulation of the nano-microstructure to construct highly ordered hierarchical structures would provide a greater possibility of simultaneously optimizing electrical and thermal properties, which would open the path toward the realization of developing high-performance thermoelectric materials.

Acknowledgments

This work was supported by the "Solid-State Solar-Thermal Energy Conversion Center (S^3TEC)," an Energy Frontier Research Center funded by the US Department of Energy, Office of Science, Office of Basic Energy Science, under Award No. DE-SC0001299.

References

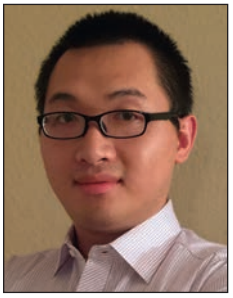
1. A.L. Moore, L. Shi, *Mater. Today* **17**, 163 (2014).
2. Z.T. Tian, S. Lee, G. Chen, *J. Heat Transfer* **135**, 061605 (2013).
3. L.D. Hicks, M.S. Dresselhaus, *Phys. Rev. B Condens. Matter* **47**, 12727 (1993).
4. L.D. Hicks, M.S. Dresselhaus, *Phys. Rev. B Condens. Matter* **47**, 16631 (1993).
5. M.S. Dresselhaus, G. Chen, M.Y. Tang, R.G. Yang, H. Lee, D.Z. Wang, Z.F. Ren, J.P. Fleurial, P. Gogna, *Adv. Mater.* **19**, 1043 (2007).
6. J. Mao, Z.H. Liu, Z.F. Ren, *NPJ Quantum Mater.* **1**, 16028 (2016).
7. G.J. Tan, L.D. Zhao, M.G. Kanatzidis, *Chem. Rev.* **116**, 12123 (2016).
8. T.J. Zhu, Y.T. Liu, C.G. Fu, J.P. Heremans, J.G. Snyder, X.B. Zhao, *Adv. Mater.* **29**, 1605884 (2017).
9. A.J. Minnich, J.A. Johnson, A.J. Schmidt, K. Esfarjani, M.S. Dresselhaus, K.A. Nelson, G. Chen, *Phys. Rev. Lett.* **107**, 095901 (2011).
10. K. Esfarjani, G. Chen, H.T. Stokes, *Phys. Rev. B Condens. Matter* **84**, 085204 (2011).
11. B. Poudel, Q. Hao, Y. Ma, Y.C. Lan, A. Minnich, B. Yu, X. Yan, D.Z. Wang, A. Muto, D. Vashaee, X.Y. Chen, J.M. Liu, M.S. Dresselhaus, G. Chen, Z.F. Ren, *Science* **320**, 634 (2008).
12. K. Biswas, J.Q. He, I.D. Blum, C.-I. Wu, T.P. Hogan, D.N. Seidman, V.P. Dravid, M.G. Kanatzidis, *Nature* **489**, 414 (2012).
13. L.D. Zhao, V.P. Dravid, M.G. Kanatzidis, *Energy Environ. Sci.* **7**, 251 (2014).
14. S.I. Kim, K.H. Lee, H.A. Mun, H.S. Kim, S.W. Hwang, J.W. Roh, D.J. Yang, W.H. Shin, X.S. Li, Y.H. Lee, G.J. Snyder, S.W. Kim, *Science* **348**, 109 (2015).
15. A.J. Minnich, M.S. Dresselhaus, Z.F. Ren, G. Chen, *Energy Environ. Sci.* **2**, 466 (2009).
16. J.H. Hong, Z.X. Hu, M. Probert, K. Li, D.H. Lv, X.N. Yang, L. Gu, N.N. Mao, Q.L. Feng, L.M. Xie, J. Zhang, D.Z. Wu, Z.Y. Zhang, C.H. Jin, W. Ji, X.X. Zhang, J. Yuan, Z. Zhang, *Nat. Commun.* **6**, 6293 (2015).
17. D. Wu, Y.L. Pei, Z. Wang, H.J. Wu, L. Huang, L.D. Zhao, J.Q. He, *Adv. Funct. Mater.* **24**, 7763 (2014).
18. J. Mao, Y. Wang, Z. Liu, B. Ge, Z. Ren, *Nano Energy* **32**, 174 (2017).
19. R. DeHoff, *Thermodynamics in Materials Science*, 2nd ed. (CRC Press, New York, 2006).
20. Y. Liu, L.D. Zhao, Y.C. Liu, J.L. Lan, W. Xu, F. Li, B.P. Zhang, D. Berardan, N. Dragoe, Y.H. Lin, *J. Am. Chem. Soc.* **133**, 20112 (2011).
21. F. Tuomisto, V. Ranki, K. Saarinen, D.C. Look, *Phys. Rev. Lett.* **91**, 205502 (2003).
22. L.P. Hu, T.J. Zhu, X.H. Liu, X.B. Zhao, *Adv. Funct. Mater.* **24**, 5211 (2014).
23. T.J. Zhu, L.P. Hu, X.B. Zhao, J. He, *Adv. Sci.* **3**, 1600004 (2016).
24. J. Callaway, H.C. von Baeyer, *Phys. Rev.* **120**, 1149 (1960).
25. J. Yang, L.L. Xi, W.J. Qiu, L.H. Wu, X. Shi, L.D. Chen, J.H. Yang, W.Q. Zhang, C. Uher, D.J. Singh, *NPJ Comput. Mater.* **2**, 15015 (2016).
26. R. He, H.T. Zhu, J.Y. Sun, J. Mao, H. Reith, S. Chen, G. Schierning, K. Nielsch, Z.F. Ren, *Mater. Today. Phys.* **1**, 24 (2017).
27. D. Hull, D.J. Bacon, *Introduction to Dislocations*, 5th ed. (Butterworth-Heinemann, Oxford, 2001).
28. D. Kuhlmann-Wilsdorf, *Mater. Sci. Eng. A* **113**, 1 (1989).
29. X.F. Meng, Z.H. Liu, B. Cui, D.D. Qin, H.Y. Geng, W. Cai, L.W. Fu, J.Q. He, Z.F. Ren, J.H. Sui, *Adv. Energy Mater.* **7**, 1602582 (2017).
30. Z.W. Chen, B.H. Ge, W. Li, S.Q. Lin, J.W. Shen, Y.J. Chang, R. Hanus, G.J. Snyder, Y.Z. Pei, *Nat. Commun.* **8**, 13828 (2017).
31. Z.W. Chen, Z.Z. Jian, W. Li, Y.J. Chang, B.H. Ge, R. Hanus, J. Yang, Y. Chen, M.X. Huang, G.J. Snyder, Y.Z. Pei, *Adv. Mater.* **29**, 1606768 (2017).
32. P.B. Hirsch, J. Silcox, R.E. Smallman, K.H. Westmacott, *Philos. Mag.* **3**, 897 (1958).
33. P. Carruthers, *Rev. Mod. Phys.* **33**, 92 (1961).
34. M.D. Li, Z.W. Ding, Q.P. Meng, J.W. Zhou, Y.M. Zhu, H. Liu, M.S. Dresselhaus, G. Chen, *Nano Lett.* **17**, 1587 (2017).
35. W.J. Xie, J. He, H.J. Kang, X.F. Tang, S. Zhu, M. Laver, S.Y. Wang, J.R. Copley, C.M. Brown, Q.J. Zhang, *Nano Lett.* **10**, 3283 (2010).
36. Z.H. Liu, W.H. Gao, X.F. Meng, X.B. Li, J. Mao, Y.M. Wang, J. Shuai, W. Cai, Z.F. Ren, J.H. Sui, *Scr. Mater.* **127**, 72 (2017).
37. X.L. Su, P. Wei, H. Li, W. Liu, Y.G. Yan, P. Li, C.Q. Su, C.J. Xie, W.Y. Zhao, P.C. Zhai, Q.J. Zhang, X.F. Tang, C. Uher, *Adv. Mater.* **29**, 1602013 (2017).
38. B.A. Cook, M.J. Kramer, X. Wei, J.L. Harringa, E.M. Levin, *J. Appl. Phys.* **101**, 053715 (2007).
39. J. Mao, Y.M. Wang, H.S. Kim, Z.H. Liu, U. Saparamadu, F. Tian, K. Dahal, J.Y. Sun, S. Chen, W.S. Liu, *Nano Energy* **17**, 279 (2015).
40. W. Gao, X. Yi, B. Sun, X. Meng, W. Cai, L. Zhao, *Acta Mater.* **132**, 405 (2017).
41. Z.H. Liu, Y.M. Wang, W.H. Gao, J. Mao, H.Y. Geng, J. Shuai, W. Cai, J.H. Sui, Z.F. Ren, *Nano Energy* **31**, 194 (2017).
42. K. Lu, *Nat. Rev. Mater.* **1**, 16019 (2016).
43. P.G. Klemens, *Int. J. Thermophys.* **15**, 1345 (1994).
44. A. Minnich, *J. Phys. Condens. Matter* **27**, 053202 (2015).
45. W.D. Callister, D.G. Rethwisch, *Materials Science and Engineering*, 4th ed. (Wiley, New York, 2011).
46. K.F. Hsu, S. Loo, F. Guo, W. Chen, J.S. Dyck, C. Uher, T. Hogan, E.K. Polychroniadis, M.G. Kanatzidis, *Science* **303**, 818 (2004).
47. J.P.A. Makongo, D.K. Misra, X.Y. Zhou, A. Pant, M.R. Shabetai, X.L. Su, C. Uher, K.L. Stokes, P.F.P. Poudeu, *J. Am. Chem. Soc.* **133**, 18843 (2011).
48. Z.H. Liu, Y.L. Pei, H.Y. Geng, J.C. Zhou, X.F. Meng, W. Cai, W.S. Liu, J.H. Sui, *Nano Energy* **13**, 554 (2015).
49. L.D. Zhao, X. Zhang, H.J. Wu, G.J. Tan, Y.L. Pei, Y. Xiao, C. Chang, D. Wu, H. Chi, L. Zheng, S.K. Gong, C. Uher, J.Q. He, M.G. Kanatzidis, *J. Am. Chem. Soc.* **138**, 2366 (2016).
50. J.Q. He, S.N. Girard, M.G. Kanatzidis, V.P. Dravid, *Adv. Funct. Mater.* **20**, 764 (2010).
51. Y. Gelbstein, B. Dado, O. Ben-Yehuda, Y. Sadia, Z. Dashevsky, M.P. Dariel, *Chem. Mater.* **22**, 1054 (2009).
52. X.F. Meng, W. Cai, Z.H. Liu, J. Li, H.Y. Geng, J.H. Sui, *Acta Mater.* **98**, 405 (2015).
53. A. Page, A. Van der Ven, P. Poudeu, C. Uher, *J. Mater. Chem. A* **4**, 13949 (2016).
54. Q. Zhang, E.K. Chere, Y.M. Wang, H.S. Kim, R. He, F. Cao, K. Dahal, D. Broido, G. Chen, Z.F. Ren, *Nano Energy* **22**, 572 (2016).
55. J.H. Li, Q. Tan, J.F. Li, D.W. Liu, F. Li, Z.Y. Li, M. Zou, K. Wang, *Adv. Funct. Mater.* **23**, 4317 (2013).
56. K.T. Kim, S.Y. Choi, E.H. Shin, K.S. Moon, H.Y. Koo, G.-G. Lee, G.H. Ha, *Carbon* **52**, 541 (2013).
57. P.A. Zong, R. Hanus, M. Dylla, Y.S. Tang, J.C. Liao, Q.H. Zhang, G.J. Snyder, L.D. Chen, *Energy Environ. Sci.* **10**, 183 (2017).
58. D.S. Smith, A. Alzina, J. Bourret, B. Nait-Ali, F. Pennec, N. Tessier-Doyen, K. Otsu, H. Matsubara, P. Elser, U.T. Gonzenbach, *J. Mater. Res.* **28**, 2260 (2013).
59. K.W. Schlichting, N.P. Padture, P.G. Klemens, *J. Mater. Sci.* **36**, 3003 (2001).
60. H. Lee, D. Vashaee, D.Z. Wang, M.S. Dresselhaus, Z.F. Ren, G. Chen, *J. Appl. Phys.* **107**, 094308 (2010).
61. A.U. Khan, K. Kobayashi, D.-M. Tang, Y. Yamauchi, K. Hasegawa, M. Mitome, Y.M. Xue, B.Z. Jiang, K. Tsuchiya, D. Golberg, Y. Bando, T. Mori, *Nano Energy* **31**, 152 (2017).
62. W. Kim, A. Majumdar, *J. Appl. Phys.* **99**, 084306 (2006).
63. A. Kundu, N. Mingo, D.A. Broido, D.A. Stewart, *Phys. Rev. B Condens. Matter* **84**, 125426 (2011).
64. H. Zhang, A.J. Minnich, *Sci. Rep.* **5**, 8995 (2015).
65. N. Zuckerman, J.R. Lukes, *Phys. Rev. B* **77**, 094302 (2008).
66. Z.T. Tian, J. Garg, K. Esfarjani, T. Shiga, J. Shiomi, G. Chen, *Phys. Rev. B Condens. Matter* **85**, 184303 (2012).
67. P.G. Klemens, *Proc. Phys. Soc. A* **68**, 1113 (1955).
68. J. Callaway, *Phys. Rev.* **113**, 1046 (1959).

https://doi.org/10.1557/mrs.2018.7 Published online by Cambridge University Press

69. Z.H. Liu, J. Mao, J.H. Sui, Z.F. Ren, *Energy Environ. Sci.* **11**, 23 (2018).
70. Z.H. Liu, Y.M. Wang, J. Mao, H.Y. Geng, J. Shuai, Y.X. Wang, R. He, W. Cai, J.H. Sui, Z.F. Ren, *Adv. Energy Mater.* **6**, 1502269 (2016).
71. K.P. Zhao, P.F. Qiu, Q.F. Song, A.B. Blichfeld, E. Eikeland, D. Ren, B.H. Ge, B.B. Iversen, X. Shi, L.D. Chen, *Mater. Today Phys.* **1**, 14 (2017).
72. F. Giustino, M.L. Cohen, S.G. Louie, *Phys. Rev. B Condens. Matter* **76**, 165108 (2007).
73. J. Sjakste, N. Vast, M. Calandra, F. Mauri, *Phys. Rev. B Condens. Matter* **92**, 054307 (2015).
74. J.F. Sun, J. Shuai, Z.F. Ren, D.J. Singh, *Mater. Today Phys.* **2**, 40 (2017).
75. T.-H. Liu, J.W. Zhou, B.L. Liao, D.J. Singh, G. Chen, *Phys. Rev. B Condens. Matter* **95**, 075206 (2017).
76. B. Qiu, Z.T. Tian, A. Vallabhaneni, B.L. Liao, J.M. Mendoza, O.D. Restrepo, X.L. Ruan, G. Chen, *Europhys. Lett.* **109**, 57006 (2015).
77. T. Luo, J. Garg, J. Shiomi, K. Esfarjani, G. Chen, *Europhys. Lett.* **101**, 16001 (2013).
78. T.-H. Liu, J.W. Zhou, M.D. Li, Z.W. Ding, Q.C. Song, B.L. Liao, L. Fu, G. Chen, *Proc. Natl. Acad. Sci. U.S.A.*, (2018) doi:10.1073/pnas.1715477115.
79. Q.C. Song, T.-H. Liu, J.W. Zhou, Z.W. Ding, G. Chen, *Mater. Today. Phys.* **2**, 69 (2017).
80. E.T. Swartz, R.O. Pohl, *Rev. Mod. Phys.* **61**, 605 (1989).
81. Z.T. Tian, K. Esfarjani, G. Chen, *Phys. Rev. B Condens. Matter* **86**, 235304 (2012).
82. E.G. Seebauer, M.C. Kratzer, *Mater. Sci. Eng. R* **55**, 57 (2006).
83. J. Mao, Y.X. Wu, S.W. Song, J. Shuai, Z.H. Liu, Y.Z. Pei, Z.F. Ren, *Mater. Today Phys.* **3**, 1 (2017).
84. Z. Liu, J. Mao, S. Peng, B. Zhou, W. Gao, J. Sui, Y. Pei, Z. Ren, *Mater. Today Phys.* **2**, 54 (2017). □



Zihang Liu is a postdoctoral fellow in the Department of Physics and TcSUH (Texas Center for Superconductivity) at the University of Houston. He received his bachelor's degree from Inner Mongolia University of Technology, China, in 2012. He obtained his PhD degree from Harbin Institute of Technology, China, in March 2017. His current research interests focus on nanostructured thermoelectric materials and devices. Liu can be reached by email at zliu48@central.uh.edu.



Jun Mao is a doctoral candidate in the Department of Mechanical Engineering at the University of Houston. He received his bachelor's degree and his master's degree in thermal and power engineering at Northeastern University, China. His current research mainly focuses on identifying novel thermoelectric materials. Mao can be reached by email at jmao5@uh.edu.



Te-Huan Liu is a postdoctoral associate in the Department of Mechanical Engineering at Massachusetts Institute of Technology (MIT). He received his BS degree in 2006 from National Central University, Taiwan, and PhD degree in 2012 from National Taiwan University, Taiwan. He has been a member of MIT's NanoEngineering Group since 2015. His research interests include carrier transport in thermoelectric materials, electron–phonon interactions, and molecular dynamics simulations. Liu can be reached by email at thliu@mit.edu.



Gang Chen is the head of the Department of Mechanical Engineering and Carl Richard Soderberg Professor of Power Engineering at Massachusetts Institute of Technology (MIT). He is also the director of the Solid-State Solar-Thermal Energy Conversion Center. He obtained his bachelor's and master's degrees from Huazhong University of Science and Technology, China, and his PhD degree from the Mechanical Engineering Department, University of California, Berkeley, in 1993. He was an assistant professor at Duke University and then a tenured associate professor at the University of California, Los Angeles, before moving to MIT. His awards include the NSF Young Investigator Award, an R&D 100 Award, and an ASME Heat Transfer Memorial Award. He is a Fellow of AAAS, APS, and ASME. In 2010, he was elected a member of the US National Academy of Engineering. Chen can be reached by phone at 617-253-3523 or by email at gchen2@mit.edu.



Zhifeng Ren is an M.D. Anderson Chair Professor in the Department of Physics and the Texas Center for Superconductivity at the University of Houston. He is experienced in materials synthesis, physics, and applications and has made seminal contributions to high-temperature superconductors; carbon nanotubes; ZnO nanowires; thermoelectric materials; nanobiomaterials and sensors; flexible transparent electrodes; hydrogen, oxygen evolution reactions, and water splitting; a 2D nanosheets for enhanced oil recovery. He has published approximately 400 journal papers and has 38 issued patents. He received and 2008 R&D 100 Award and the 2014 Edith and Peter O'Donnell Award from The Academy of Medicine, Engineering & Science of Texas. He is Fellow of APS, AAAS, and NAI. Ren can be reached by phone at 713-743-8217 or by email at zren@uh.edu.



https://doi.org/10.1557/mrs.2018.7 Published online by Cambridge University Press